Available online at www.sciencedirect.com

ScienceDirect

Ceramics International 40 (2014) 2885–2890

CERAMICS INTERNATIONAL

www.elsevier.com/locate/ceramint

Influence of annealing temperature on the structural and anti-corrosion characteristics of sol–gel derived, spin-coated thin films

E. Salahinejad[a,b,c,*], M.J. Hadianfard[c], D. Vashaee[d], L. Tayebi[b,e,**]

[a]Faculty of Materials Science and Engineering, K.N. Toosi University of Technology, Tehran, Iran
[b]School of Materials Science and Engineering, Helmerich Advanced Technology Research Center, Oklahoma State University, Tulsa, OK, USA
[c]Department of Materials Science and Engineering, School of Engineering, Shiraz University, Shiraz, Iran
[d]School of Electrical and Computer Engineering, Helmerich Advanced Technology Research Center, Oklahoma State University, Tulsa, OK, USA
[e]School of Chemical Engineering, Oklahoma State University, Stillwater, OK, USA

Received 16 September 2013; received in revised form 5 October 2013; accepted 5 October 2013
Available online 12 October 2013

Abstract

Recently, an aqueous particulate sol–gel process using metallic chloride precursors was introduced to synthesize zirconium titanate. In this paper, the effect of annealing temperature on the structural and corrosion protection characteristics of spin-coated thin films obtained from this sol–gel system was investigated. Based on scanning electron microscopy, transmission electron microscopy, atomic force microscopy, and spectroscopic reflectometry studies, it was found that the flatness and thickness of the thin films were decreased by increasing the annealing temperature. Also, the corrosion protection of stainless steel AISI 316L provided by the prepared coatings, as analyzed by electrochemical potentiodynamic polarization experiments in a simulated body fluid, was improved in this order: 500 °C-annealed sample < 900 °C-annealed sample < 700 °C-annealed sample, attributed to a compromise between the defect density and the adhesion of the films to the substrate.

Keywords: A. Sol–gel processes; C. Corrosion; E. Biomedical applications

1. Introduction

Zirconium titanate, with the orthorhombic α-PbO_2 type structure, is one of the most promising ceramics for electronic, optical, catalytic, chemical, and biomedical applications [1–3]. One of the successful methods to produce powders of this material is the sol–gel approach, where the synthesized amorphous structures crystallize at temperatures considerably lower than those obtained by other routes [4–6]. High homogeneity (because of atomic-scale mixing), low sintering temperatures (owing to nano-sized particles), and coating simplicity of complex shapes are the typical advantages of this method.

Sol–gel synthesis can be performed by hydrolysis and condensation of inorganic salts or alkoxides. The procedures starting from the former precursors are categorized as the particulate sol–gel processes, in which nanoparticles are directly synthesized and then dispersed in the medium. Recently, a successful particulate sol–gel method using metallic chloride precursors was introduced to synthesize zirconium titanate [7]. The typical advantage of this method is the opportunity of using relatively low-cost chlorides, rather than expensive alkoxide precursors. In the literature, the structural and surface characteristics of monolayer and multilayer coatings obtained from the aforementioned nanoparticles uniformly-dispersed in an aqueous solution using carboxymethyl cellulose, after heat-treating at 700 °C, have been reported [8–11]. Moreover, the corrosion behavior and biocompatibility of stainless steels coated with the above-mentioned coating, in the forms of pure oxide and hybrid, have been investigated [12,13].

This work evaluates the influence of annealing temperature (500, 700, and 900 °C) on the structural and corrosion protection

*Corresponding author at: Faculty of Materials Science and Engineering, K.N. Toosi University of Technology, Tehran, Iran. Tel.: +98 917 387 9390.
**Corresponding author at: Helmerich Advanced Technology Research Center, School of Materials Science and Engineering, Oklahoma State University, OK, USA. Tel.: +1 918 594 8634.
E-mail addresses: salahinejad@kntu.ac.ir, erfan.salahinejad@gmail.com (E. Salahinejad), lobat.tayebi@okstate.edu (L. Tayebi).

0272-8842/$ - see front matter © 2013 Elsevier Ltd and Techna Group S.r.l. All rights reserved.
http://dx.doi.org/10.1016/j.ceramint.2013.10.023

properties of zirconium titanate nanoparticles and thin films prepared by the above-mentioned sol–gel process.

2. Experimental work

2.1. Coating preparation and characterization

An equal-molar solution of $ZrCl_4$ (Alfa Aesar, 99.5%) and $TiCl_4$ (Alfa Aesar, 99.99%) was prepared in deionized water, which led to a pH value of almost 1. Then, by the dropwise addition of a NaOH solution, the pH of the solution was increased to 7. The obtained hydrogels were rinsed several times with deionized water to remove chloride ion. After adding 2 wt% carboxymethyl cellulose (CMC, sodium salt, Alfa Aesar) as a dispersing agent [8], films were spin-coated on surface-prepared stainless steel AISI 316L substrates at 3000 rpm. The obtained films were then annealed at 500, 700, and 900 °C for 1 h.

To evaluate the variation of the powder particles constituting the films, the powder samples heat-treated with the same thermal cycles were studied by a transmission electron microscope (TEM, JEOL JEM-2100, 200 kV). The film surfaces were then studied by a field emission scanning electron microscope (SEM, Hitachi S-4800) and Veeco Multimode atomic force microscope (AFM, Bruker AXS). The film thickness was also measured by a NanoSpec 3000 system (Nanometrics, CA, USA).

2.2. Electrochemical corrosion characterization

The corrosion behavior of the coated samples was investigated in the simulated body fluid [14] with the pH value of 7.4. To do so, a platinum wire and saturated calomel electrode (SCE) were used as auxiliary and reference electrodes, respectively. Anodic potentiodynamic polarization curves were obtained at a scan rate of 1 m V s^{-1} from −0.1 V vs. *ocp* to the transpassive potential. The specimen surfaces that failed

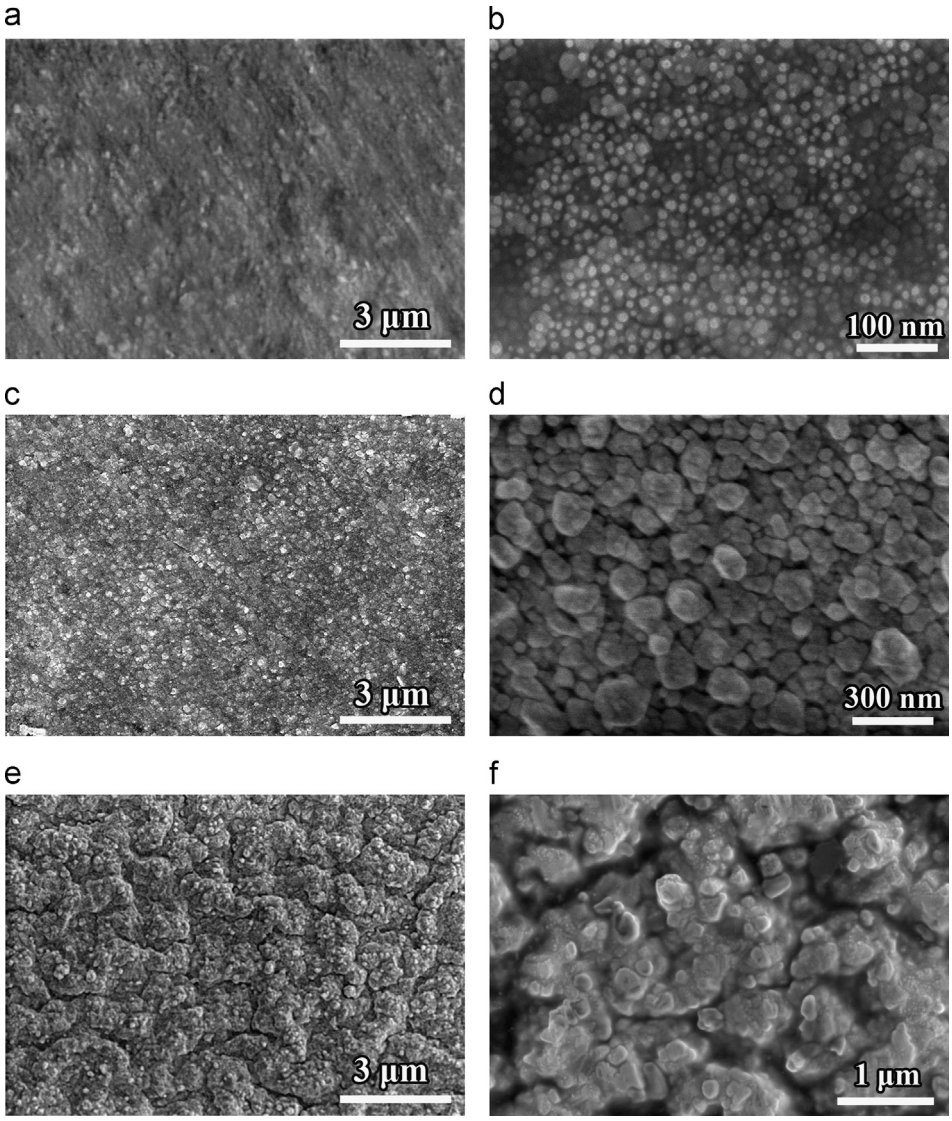

Fig. 1. SEM micrographs of the films annealed at 500 °C (a and b), 700 °C (c and d), and 900 °C (e and f) in two magnifications.

due to the polarization tests were also studied by SEM. Moreover, the film adhesion to the substrate was evaluated by the adhesive tape test (ASTM D 3359).

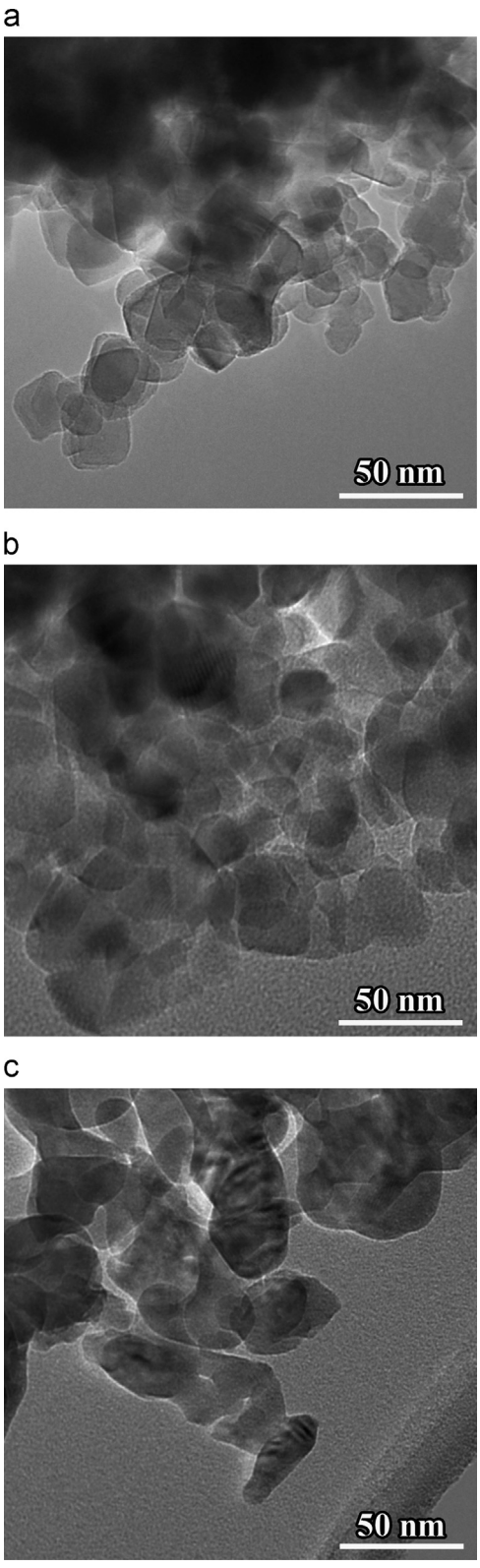

Fig. 2. TEM micrographs of the powder annealed at 500 °C (a), 700 °C (b), and 900 °C (c).

3. Results and discussion

3.1. Effect of annealing temperature on the surface characteristics

Fig. 1 indicates the SEM micrograph of the films heat-treated at 500, 700, and 900 °C. It can be seen that relatively dense, smooth, well-covering, and uniform coatings have been produced. These desirable features of the films are owing to the presence of CMC in the sol as a particle dispersing agent and also the merit of the deposition and firing processes allowing the gradual removal of volatile materials [8]. The nanoparticulate nature of the coatings is also evident in the higher magnification SEM micrographs represented in Fig. 1, where the surfaces of the specimens annealed at 500, 700, and 900 °C are composed of particles/clusters with the average sizes of about 20, 90, and 200 nm, respectively. On the other hand, in the SEM micrographs, a decrease of flatness is observed by increasing the annealing temperature, as detailed below by the AFM studies.

As it is basically difficult to distinguish particles from clusters by SEM, especially in the nano-metric scale, the powder samples annealed with the same thermal cycles used for the coatings were studied by TEM (Fig. 2). As can be seen, the average particle size of the samples annealed at 500, 700, and 900 °C is almost 15, 50, and 80 nm, respectively. This analysis infers particle growth with increasing the annealing temperature, due to the tendency to decrease surface energy. According to Fig. 3 which depicts the results of the spectroscopic reflectometer, the film thickness is slightly decreased by increasing the annealing temperature, because of the domination of sintering, shrinkage, and densification of the deposited nanoparticles.

Fig. 4 shows the two- and three-dimensional AFM pictures of the films heat-treated at 500, 700, and 900 °C. The average roughness value of the films over areas of $10 \times 10\ \mu m^2$ is presented in Fig. 5. It can be seen that by increasing the annealing temperature, the roughness is increased, as qualitatively observed in the SEM and AFM micrographs. Note that to provide contrast to the two- and three-dimensional AFM images, the scale bars and height scales have been presented differently.

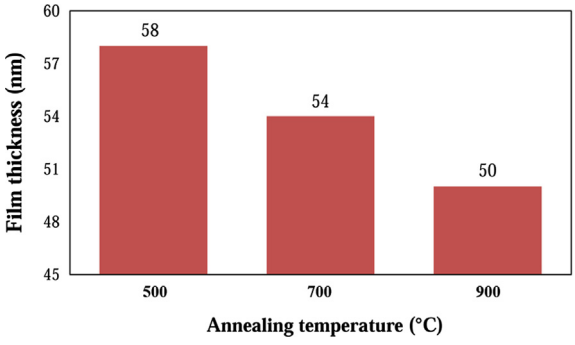

Fig. 3. Results of the coating thickness measured by the spectroscopic reflectometer.

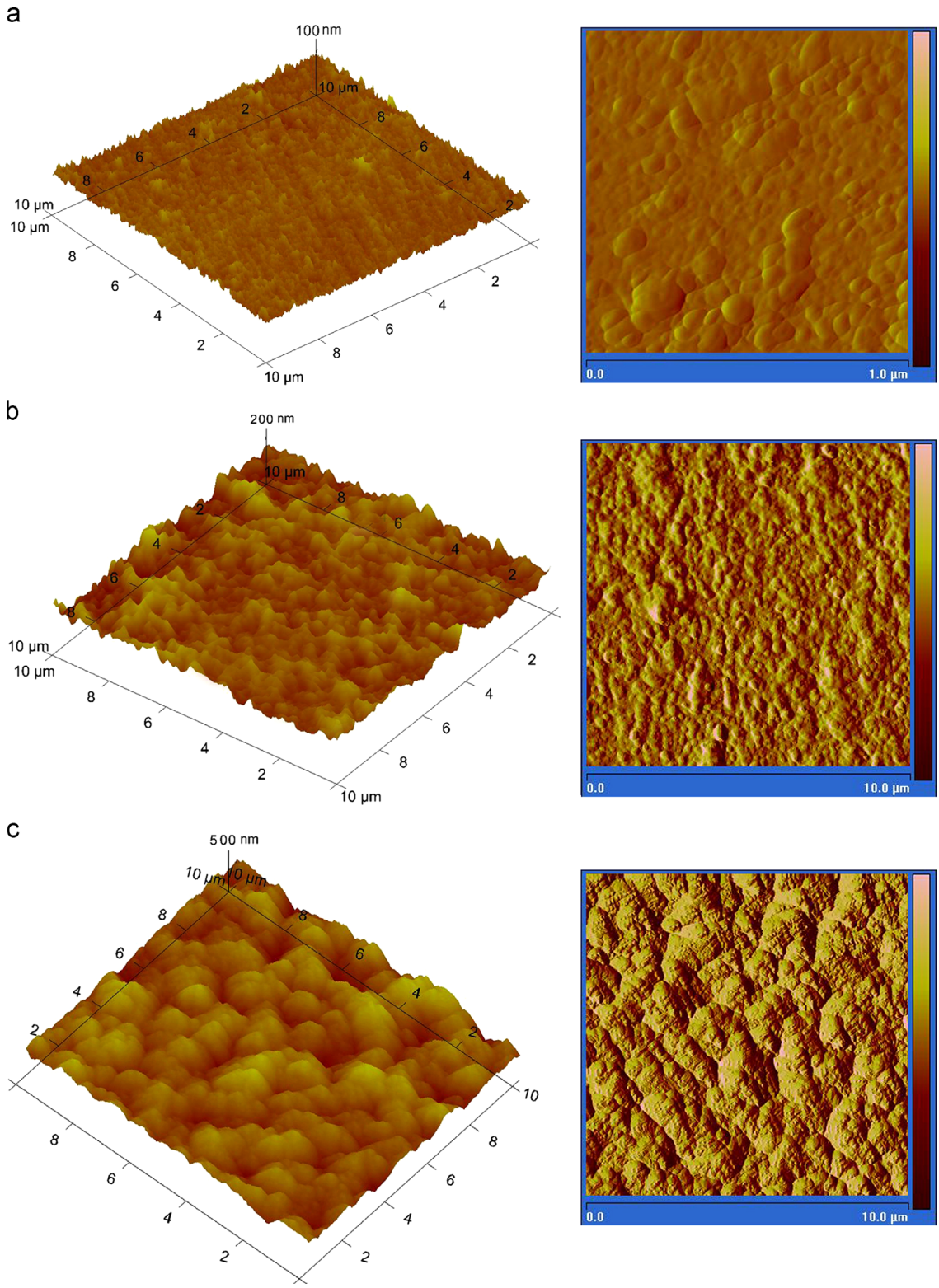

Fig. 4. AFM pictures of the films heat-treated at 500 °C (a), 700 °C (b), and 900 °C (c).

In the course of sintering, the nanoparticles grow and appear on the surface, due to a mass transfer governed by the glass-to-crystalline phase transformation [15]. In other words, the strain of the initially-formed layer is released by the development of three-dimensional islands (Stranski–Krastanov growth model) [16], thereby making films rough. Clearly, the aforementioned mechanisms proceed more effectively and faster by increasing the annealing temperature, which justifies the observed variation in the roughness value. In other words, because of the progress in nanoparticle growth with increasing temperature,

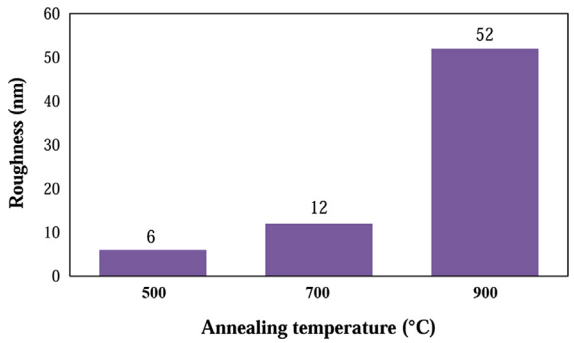

Fig. 5. Average roughness values of the coatings annealed at the different temperatures.

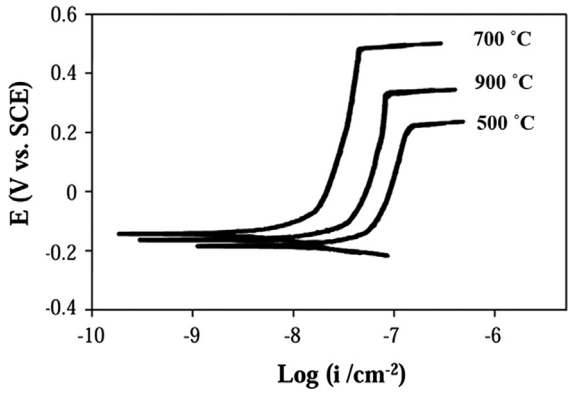

Fig. 6. Potentiodynamic polarization curves of the coated samples annealed at the different temperatures.

the coatings processed at 500, 700, and 900 °C consist of globular nanoparticles with the average diameters of 30, 50, and 150 nm, respectively, as signified in the microscopic images.

3.2. *Effect of annealing temperature on the anti-corrosion performance of the coatings*

Fig. 6 presents the electrochemical polarization curve of the coated samples. As can be seen, from the viewpoints of corrosion potential, corrosion current density, passivity, and passive potential range, the corrosion protection of the stainless steel substrate by the coatings is improved in the following annealing temperatures: 500 °C sample < 900 °C sample < 700 °C sample. The inferior corrosion resistance of the sample annealed at 500 °C, compared with the other two specimens, is attributed to its low sintering temperature which provides a highly-porous coating. This coating structure cannot efficiently impede the electrolyte access to the metal surface via existing physical defects.

However, the coating annealed at 700 °C presents a better corrosion protection compared with that annealed at 900 °C, although the latter has a lower porosity level because of the higher sintering temperature used. This unexpected trend originates from the dominating role of the film adhesion to the substrate, where the adhesions of the coatings annealed at 700 and 900 °C were rated as 5B (desirable adhesion) and 4B

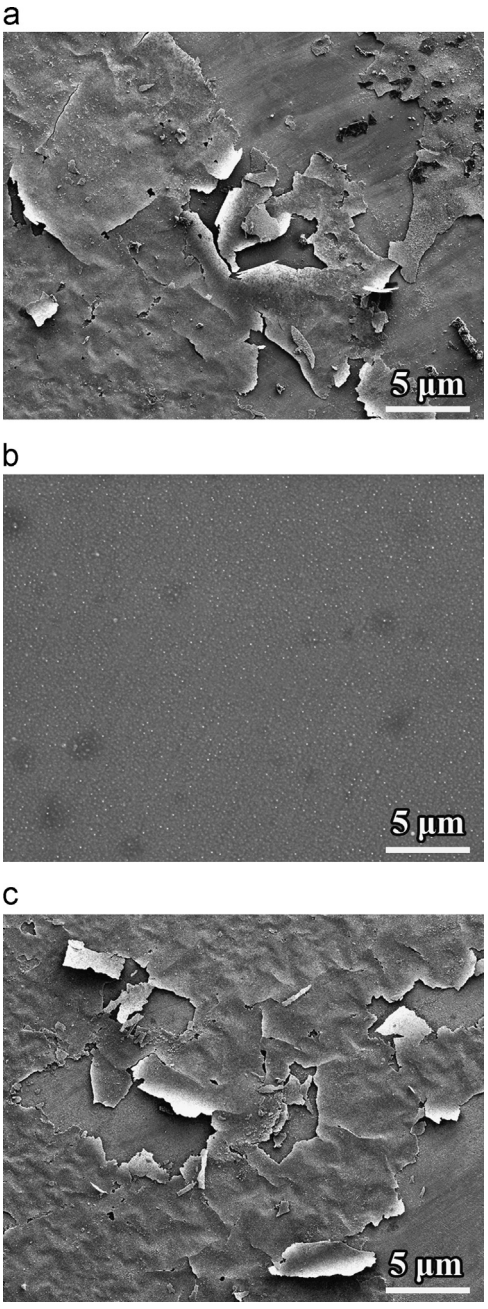

Fig. 7. SEM micrographs of the surfaces of the samples annealed at 500 °C (a), 700 °C (b), and 900 °C (c) after the polarization tests.

(slightly weaker adhesion than 5B), respectively. Oxygen-bonding between the substrate and the coating is responsible for the adhesion of both of the coatings [17]. Nevertheless, because of the different thermal expansion coefficients of the substrate and coating materials, the possibility of the formation of defects in the interface and thereby the weakening of the film adhesion are increased by increasing the annealing temperature from 700 °C to 900 °C. A consideration to the surfaces that failed after the corrosion tests also suggests that debonding and delamination for the sample prepared at 900 °C are more dramatic than those for the sample prepared at 700 °C (Fig. 7), where the evolution of electrochemical processes

under the film with the weaker adhesion has promoted these features.

4. Summary

This paper investigated the effect of annealing temperature on the structural and corrosion protection properties of sol–gel derived zirconium titanate thin films. It was found that by increasing the annealing temperature, the mean roughness value of the deposited thin films was increased, while the film thickness was decreased. The corrosion protection provided by the coatings was improved in the following order: 500 °C sample < 900 °C sample < 700 °C sample, as attributed to a compromise between the defect density and the adhesion of the films to the substrate.

Acknowledgments

This work was partially supported by AFOSR under Grant no. FA9550-10-1-0010, the National Science Foundation (NSF) under Grant no. 0933763, and Oklahoma Center for Advancement of Science and Technology under Grant no. AR131-054 8161.

References

[1] M.Z.C. Hu, E.A. Payzant, K.R. Booth, C.J. Rawn, R.D. Hunt, L.F. Allard, Ultrafine microsphere particles of zirconium titanate produced by homogeneous dielectric-tuning coprecipitation, J. Mater. Sci. 38 (2003) 3831–3844.

[2] L. Pandolfi, S. Kaciulis, G. Padeletti, A. Cusma, M. Viticoli, Deposition and characterization of $ZrTiO_4$ thin films, Surf. Interf. Anal. 36 (2004) 1159–1162.

[3] D.V. Shtansky, M.I. Petrzhik, I.A. Bashkova, F.V. Kiryukhantsev-Korneev, A.N. Sheveiko, E.A. Levashov, Adhesion, friction, and deformation characteristics of Ti–(Ca,Zr)–(C,N,O,P) coatings for orthopedic and dental implants, Phys. Solid State 48 (2006) 1301–1308.

[4] L.G. Karakchiev, T.M. Zima, N.Z. Lyakhov, Low-temperature synthesis of zirconium titanate, Inorg. Mater. 37 (2001) 386–390.

[5] L.Y. Zhu, D. Xu, G. Yu, X.Q. Wang, Preparation and characterization of zirconium titanate fibers with good high temperature performance, J. Sol–Gel Sci. Technol. 49 (2009) 341–346.

[6] J. Macan, A. Gajovi, H. Ivankovic, Porous zirconium titanate ceramics synthesized by sol–gel process, J. Eur. Ceram. Soc. 29 (2009) 691–696.

[7] E. Salahinejad, M.J. Hadianfard, D.D. Macdonald, I. Karimi, D. Vashaee, L. Tayebi, Aqueous sol–gel synthesis of zirconium titanate ($ZrTiO_4$) nanoparticles using chloride precursors, Ceram. Int. 38 (2012) 6145–6149.

[8] E. Salahinejad, M.J. Hadianfard, D.D. Macdonald, M. Mozafari, D. Vashaee, L. Tayebi, Zirconium titanate thin film prepared by an aqueous particulate sol–gel spin coating process using carboxymethyl cellulose as dispersant, Mater. Lett., 88, 2012, p. 5–8.

[9] E. Salahinejad, M.J. Hadianfard, D.D. Macdonald, M. Mozafari, D. Vashaee, L. Tayebi, Multilayer zirconium titanate thin films prepared by a sol–gel deposition method, Ceram. Int. 39 (2013) 1271–1276.

[10] P. Rouhani, E. Salahinejad, R. Kaul, D. Vashaee, L. Tayebi, Nano structured zirconium titanate fibers prepared by particulate sol-gel and cellulose templating techniques, J. Alloys Compd. 568 (2013) 102–105.

[11] M. Mozafari, E. Salahinejad, V. Shabafrooz, M. Yazdimamaghani, D. Vashaee, L. Tayebi, Multilayer bioactive glass/zirconium titanate thin films for bone tissue engineering and regenerative dentistry, Int. J. Nanomed. 8 (2013) 1665–1672.

[12] E. Salahinejad, M.J. Hadianfard, D.D. Macdonald, M. Mozafari, D. Vashaee, L. Tayebi, A new double-layer sol–gel coating to improve the corrosion resistance of a medical-grade stainless steel in a simulated body fluid, Mater. Lett. 97 (2013) 162–165.

[13] E. Salahinejad, M.J. Hadianfard, D.D. Macdonald, S. Sharifi-Asl, M. Mozafari, K.J. Walker, A. Tahmasbi Rad, S.V. Madihally, D. Vashaee, L. Tayebi, Surface modification of stainless steel orthopedic implants by sol–gel $ZrTiO_4$ and $ZrTiO_4$–PMMA coatings, J. Biomed. Nanotechnol. 9 (2013) 1327–1335.

[14] T. Kokubo, H. Takadama, How useful is SBF in predicting in vivo bone bioactivity?, Biomaterials 27 (2006) 2907–2915.

[15] S. Satapathy, P. Verma, P.K. Gupta, C. Mukherjee, V.G. Sathe, K.B.R. Varma, Structural, dielectric and ferroelectric properties of multilayer lithium tantalate thin films prepared by sol–gel technique, Thin Solid Films 519 (2011) 1803–1808.

[16] J.W. Matthews, in: J.W. Matthews (Ed.), Epitaxial Growth, Academic Press, New York, 1975, p. 566.

[17] J.M. Yeh, C.J. Weng, W.J. Liao, Y.W. Mau, Anticorrosively enhanced PMMA–SiO_2 hybrid coatings prepared from the sol–gel approach with MSMA as the coupling agent, Surf. Coat. Technol. 201 (2006) 1788–1795.